Supporting information.

The attached movies are as follows:

Left.front.mpg = movie of cellulose Iβ edge chain decrystallization (front view)

Left.side.mpg = movie of cellulose Iβ edge chain decrystallization (side view)

Equilibration simulations

Table S1. Root mean square fluctuations of the chains of interest during the 10 ns equilibration averaged over the entire chain.

Chain of interest	RMSF μ	RMSF σ
Iβ edge	0.700	0.153
Iβ middle	0.592	0.137
Iβ corner	0.792	0.205
Iα edge	0.749	0.231
Iα middle	0.585	0.176
II edge	1.134	0.460
III_I edge	1.809	0.386

As with the hydrogen bonds and the RMSF of the chains of interest, we calculated the primary alcohol conformations (from the dihedral angle of O5-C5-C6-O6) over the last 8 ns of the equilibration simulations, as shown in Figure S1. From left to right, the conformations are gauche-gauche (GG) which is centered around -60º, gauche-trans (GT) which is centered around 60º, and trans-gauche (TG) which is centered around 180º. As shown for cellulose Iβ, there is a significant increase in the number of GT conformations in the corner chain, and a slight difference in GG and TG conformations between the edge and middle chains. For cellulose Iα, there are very few residues in the GG conformation in either the edge or middle chain, which is quite different from cellulose Iβ. For both natural polymorphs in all cases, there is a considerable shift from the TG conformation expected from the experimental structures. The cellulose II and III_I edge chains are predominantly in the GT conformation.

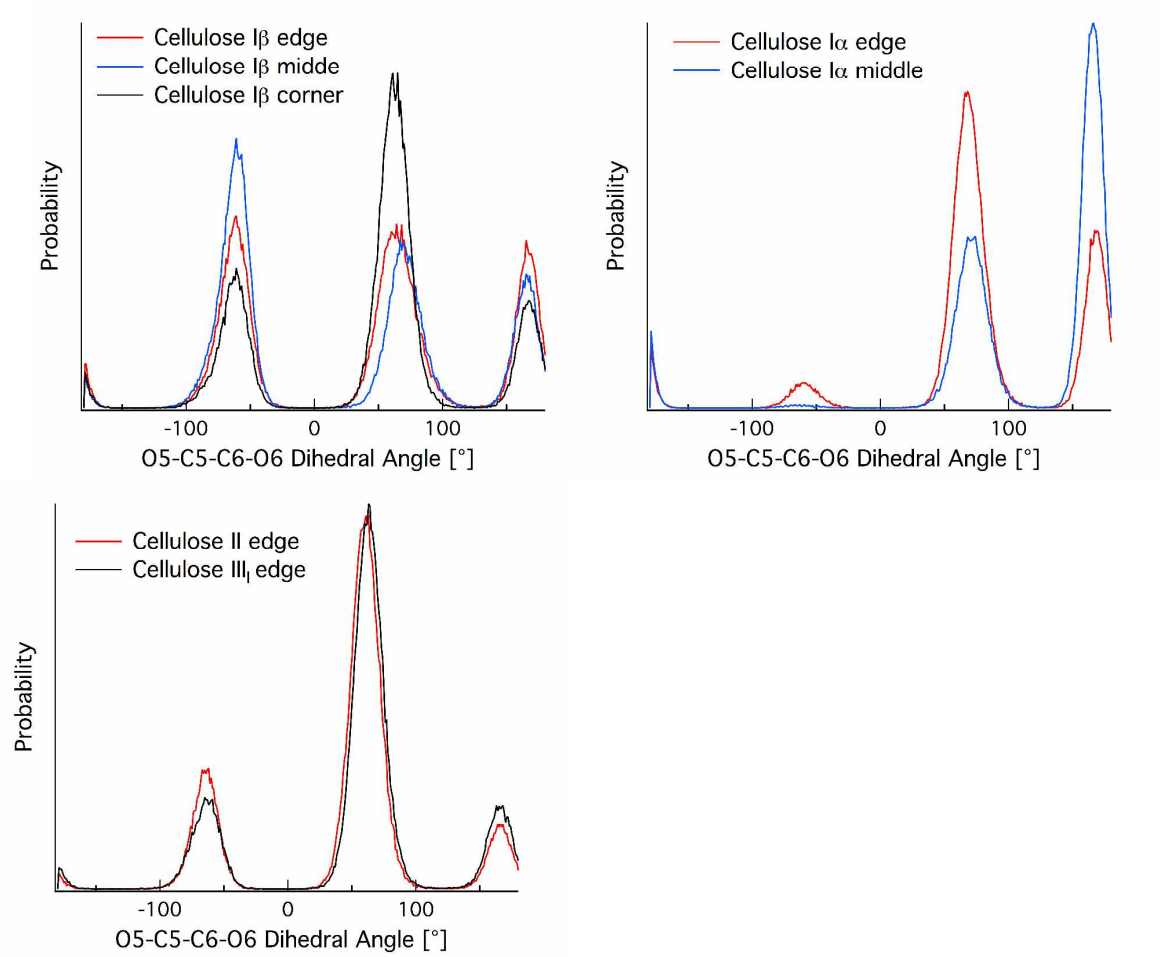

Figure S1. Primary alcohol conformation histograms for the chains of interest over the last 8 ns of equilibration.

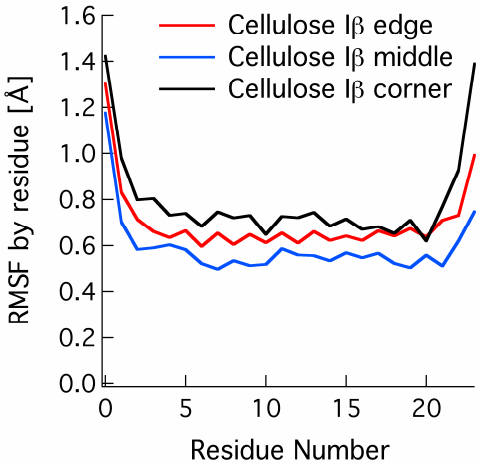

Figure S2. Root mean square fluctuations of edge and middle chains in cellulose Iβ during the 8 ns equilibration. This figure illustrates that the ends of the cellulose microfibrils exhibit significant fluctuations, which will affect the inflection in the work profiles.

Decrystallization simulations.
Figure S3 shows the change in SASA for each scenario:

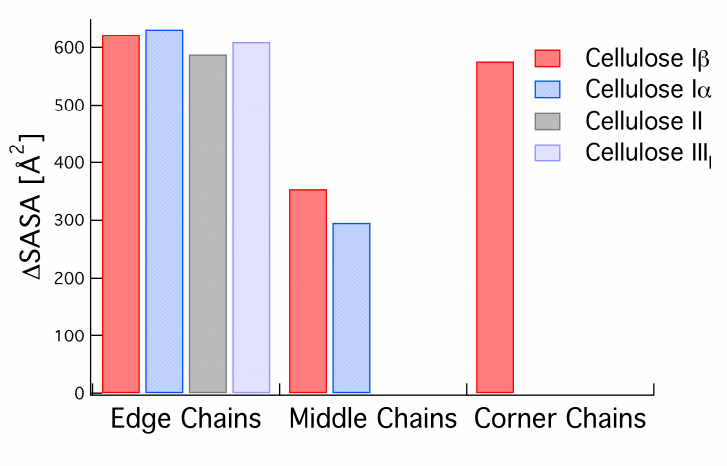

Figure S3. The change in solvent accessible surface area during the decrystallization trajectories.

The change in SASA was calculated with a probe volume of 1.4 Å over the decrystallization trajectories, and the chains considered were those directly adjacent to the chain of interest being decrystallized. As the SASA profiles were approximately linear, we fit lines to the SASA profile and from these fits, determined the change in SASA.

We calculated the mass-weighted occupancy of the chains during the decrystallization trajectories to determine if the conformational space searched affected the differences in intrinsic work (i.e., the entropic component). The occupancy or volume sampled was calculated based on a 1% threshold for the heavy atoms in the cellulose chain. A primary hypothesis for the edge and middle chains is that the middle chains should be more sterically hindered, and thus entropic contributions would increase the work of decrystallization over edge chains. Figure S4 shows the mass-weighted occupancy of the cellulose chain during decrystallization.

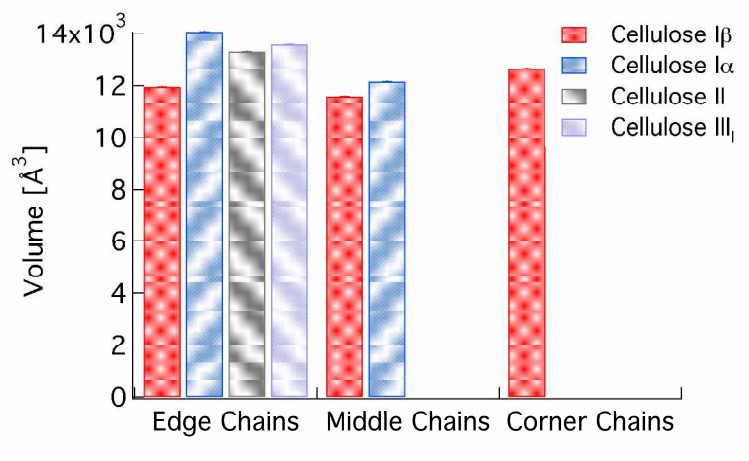

Figure S4. The mass weighted occupancy for the cellulose chains during decrystallization.

From Figure S4, there are several interesting things to note. In the cellulose Iβ edge and middle chains, the occupancy is lower than the same chains in cellulose Iα, although the difference is small around 10-15%. Moreover, the cellulose II and III_I chains are comparable to those in the edge chains of cellulose Iβ and Iα. The corner chain, as expected, has a slightly higher occupancy volume than either the edge or middle chain in cellulose Iβ. It is likely that the reduced conformational sampling exhibited in cellulose Iβ relative to cellulose Iα will contribute small differences to the entropic component of the different decrystallization work between these two polymorphs.

In all cases we calculated the RMSF of the chains that were directly adjacent to the decrystallized chain. The data in Figure S5 are the differences of the RMSF averaged over the 410 ns decrystallization trajectories from the RMSF averaged from the equilibration trajectories for adjacent chains for each scenario. In all cases, the chains are shown with the same color as the curves on the graphs. The primary hypothesis in investigating this quantity is that the magnitude of the fluctuations of the adjacent chains exposed during decrystallization may contribute entropically to the decrystallization work. There are several interesting results in Figure S5. As observed in the decrystallization trajectories, the RMSF for the chains at the end of the microfibril display the most deviation during the decrystallization trajectories. This is quite significant in cellulose III_I where both the chain below and the chain beside the chain of interest display approximately an RMSF of 0.7 to 0.9 Å. In cellulose II, however, the adjacent chains surprisingly display almost no deviation from the equilibration trajectories. Within the Iβ and Iα edge chains, the adjacent intra-layer chains, not surprisingly from the hydrogen bond information in Table 1, display the most fluctuations whereas the two chains in the layer below display almost no difference in fluctuations from the equilibration trajectories.

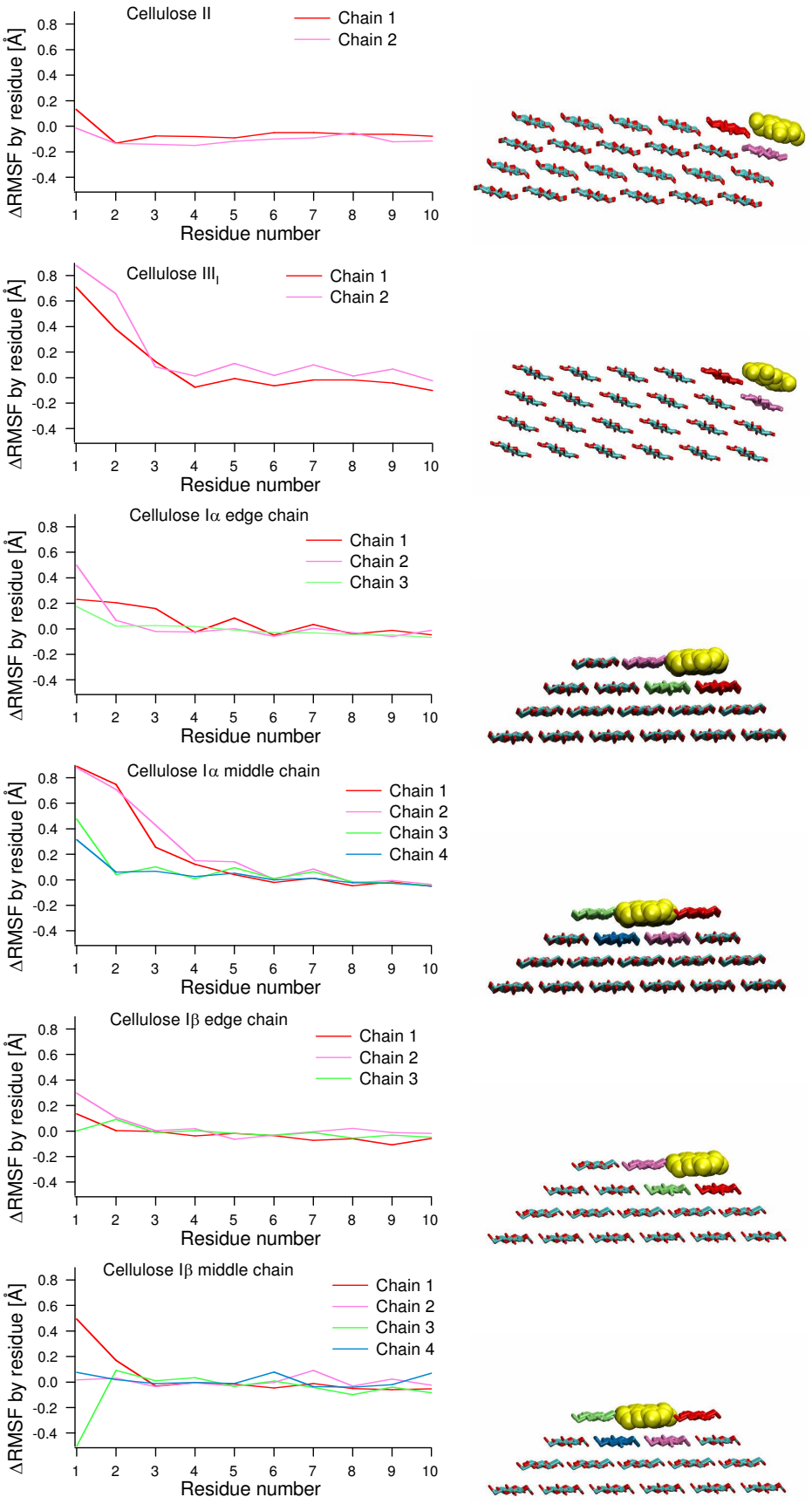
Cellulose II
Chain 1
Chain 2
ΔRMSF by residue [Å]
Residue number
Cellulose III$_I$
Chain 1
Chain 2
ΔRMSF by residue [Å]
Residue number
Cellulose Iα edge chain
Chain 1
Chain 2
Chain 3
ΔRMSF by residue [Å]
Residue number
Cellulose Iα middle chain
Chain 1
Chain 2
Chain 3
Chain 4
ΔRMSF by residue [Å]
Residue number
Cellulose Iβ edge chain
Chain 1
Chain 2
Chain 3
ΔRMSF by residue [Å]
Residue number
Cellulose Iβ middle chain
Chain 1
Chain 2
Chain 3
Chain 4
ΔRMSF by residue [Å]
Residue number

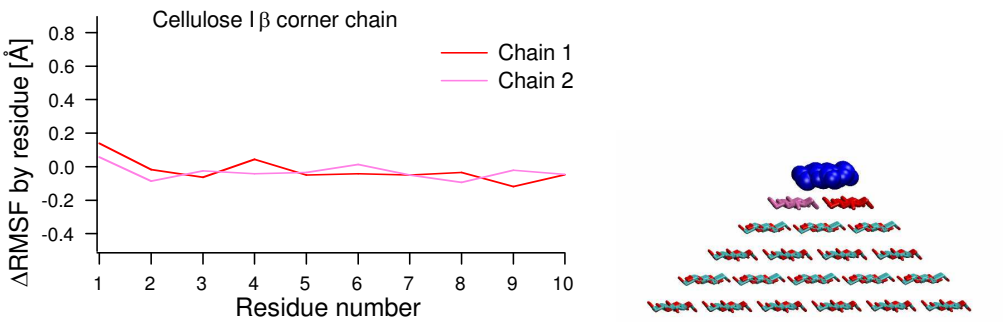

Figure S5. The change in the RMSF between the decrystallization trajectories and the equilibration trajectories.